

Effect of Calcination Temperature on the Structural Properties of Spinel $\text{Li}_4\text{Ti}_5\text{O}_{12}$ Anode Material for Lithium-Ion Batteries

B. VIKRAM BABU^{1*}, G. TEWODROS AREGAI¹,
K. VIJAYA BABU², K. SAMATHA¹ and V. VEERAAIAH¹

¹Department of Physics, Andhra University, Visakhapatnam, India

²Advanced Analytical Laboratory, Andhra University, Visakhapatnam, India
vikramphdau@gmail.com

Received 28 October 2016 / Accepted 7 November 2016

Abstract: Spinel $\text{Li}_4\text{Ti}_5\text{O}_{12}$ (LTO) was synthesized by solid state reaction method and the effect of calcination temperature on structural characteristics was investigated. Thermal analysis reveals the temperature dependence of the materials properties. The phase composition, morphology, elemental analysis and Wyckoff sites of the material is characterized by x-ray diffraction (XRD), scanning electron microscopy (SEM), energy dispersive spectra (EDS) and Fourier transform infrared (FT-IR) spectra respectively. The results of XRD pattern possessed cubic spinel $\text{Li}_4\text{Ti}_5\text{O}_{12}$ structure with space group $\text{Fd}3\text{m}$. The morphological features of the powders are ranging from $0.91\mu\text{m}$ - $1.5\mu\text{m}$. The EDS spectra confirm the presence of Ti and O in the compound. The FT-IR spectroscopic data reveals that the structure of the oxide lattice constituted by LiO_6 and TiO_6 octahedra. From this study, we conclude that the spinel $\text{Li}_4\text{Ti}_5\text{O}_{12}$ material prepared by solid-state reaction method at different temperature is that the maximum and minimum intensity ratios of XRD spectra and the JCPDS results shows that the optimum calcination temperature is 900°C for 16 h.

Keywords: Spinel structure, XRD, SEM, EDS, FT-IR

Introduction

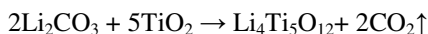
The spinel-type lithium titanate ($\text{Li}_4\text{Ti}_5\text{O}_{12}$) are gaining more and more attention as anode materials applied in solid-state lithium ion batteries^{1,2}. As extensively reported, the main feature of the compounds is their unique insertion and de-insertion mechanism that involves a two-phase process between two compounds having the same symmetry. The appearance of lithium-ion batteries has changed the human daily life-style significantly, which was widely used as the key energy component of the digital products in today's information society due to the advantages of higher energy density, higher working voltage and even the friendliness toward the environment³⁻⁵. In order to meet the demand of electric vehicles (EV) on power sources, many efforts have been made to develop new active electrode materials with high specific energy density and excellent power performance⁶. Graphite- based material was

commonly used as the anode material in the state of the art lithium-ion batteries due to its desirable charge potential profile, good cycleability and safety features. However, it suffers from the poor rate capability, co-intercalation of solvated lithium ion due to its layered structural characteristics, and lower lithiation potential (close to 0 V *vs.* Li⁺/Li). Which may cause the dendritic deposition of metal lithium on the electrode surface if the batteries are over-charged, limiting the application in power battery for EV development⁷. Therefore, searching for alternative anode materials with excellent rate-capability and good safety property has become the main topic in the battery research field. Many new anode materials have been proposed and extensively investigated, such as Sn-based, Sb-based and Si-based materials⁸⁻¹¹, various transition metal oxides¹²⁻¹⁶, hard carbons^{8,17} and Li₄Ti₅O₁₂. In particular, Li₄Ti₅O₁₂ is of interest as the anode material for lithium-ion batteries used for EV and energy storage devices owing to its favourable characteristics, including good structure stability ("zero strain" material) during lithium insertion/extraction process and higher flat electrode reaction voltage (1.55 V *vs.* Li⁺/Li). The former ensures the long-term cycling stability, while the latter enables the reliable safety^{2,18,19}.

The aim of this work is to synthesize Li₄Ti₅O₁₂ anode material by solid state reaction method with different calcination temperatures, 850/12 h (LTO-1), 850/16 h (LTO-2), 950/16 h (LTO-3) and 900 °C/16 h (LTO-4) and to identify the effects of calcination temperature on the properties of the synthesized anode material and optimize the calcination temperature.

Experimental

The anode material is synthesized by a solid-state reaction method from stoichiometric amounts of Li₂CO₃ (Sigma Aldrich 99.9%), TiO₂ (Sigma Aldrich 99.9%) as



A slight excess amount of lithium (5%) was used to compensate for any loss of the metal which might have occurred during the calcination process. The solid state reaction synthesis method involves one step. The precursors, as raw materials are well mixed and thoroughly ground with agate mortar, then subjected to heat treatment and calcined at different temperature to dry the samples free from impurities. Finally, the mixture powder is calcined at different temperatures, 850 °C for 12 h, 850 °C, 900 °C and 950 °C for 16 h to complete the chemical reaction in air using a muffle box furnace.

The TG/DTG measurement are conducted using Mettler Toledo TG 851^o instrument from room temperature to 1000 °C in Nitrogen atmosphere at a heating rate of 10 °C /min. The powder x-ray diffraction (XRD) data of the sample is collected on a PANalytical x-pert pro diffractometer with diffraction angles of 10° and 90° in increments of 0.02°. The unit cell lattice parameter is obtained by the unit cell software from the 2θ and (hkl) values. Further, the crystallite size of the sample is obtained by applying the Scherrer's equation from XRD pattern. The particle morphology and elemental analysis of the powders are observed using scanning electron microscopy (SEM) and energy dispersive spectra (EDS) taken from JEOL JSM-6610LV connected with INCA energy 250, Oxford. Fourier transform infrared (FT-IR) spectra are obtained on a Shimadzu IR-Prestige21 spectrometer using KBr pellet technique in the wave number range between 400 and 2000 cm⁻¹.

Results and Discussion

Thermal analysis

In order to investigate the possible reactions occurring in the synthesis of Li₄Ti₅O₁₂, thermo gravimetric analysis is conducted on the precursor in N₂ atmosphere shown in Figure 1.

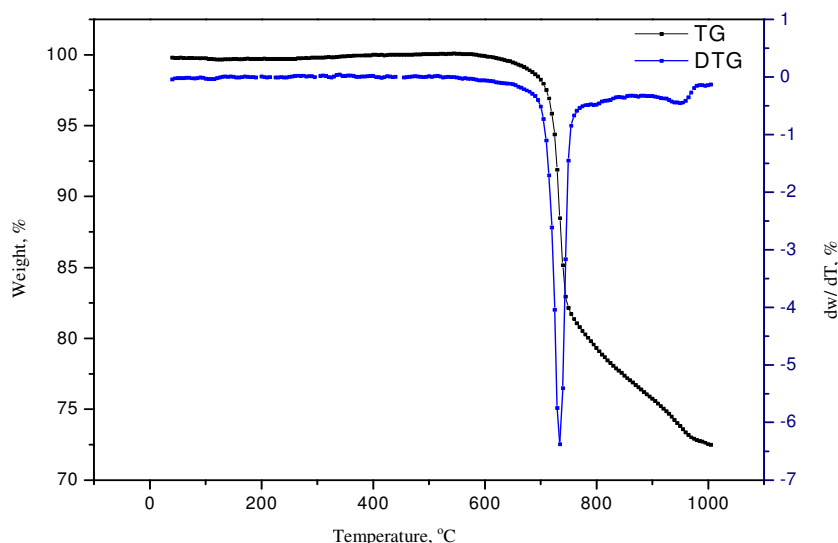


Figure 1. TG/DTG curve for $\text{Li}_4\text{Ti}_5\text{O}_{12}$ sample

There is no weight loss from room temperature to 620 °C as can be observed from the curve. The first step of mass loss about 2% occurred between 620 °C and 710 °C can be assigned to the loss of water adsorbed on the surfaces and some intercalated water molecules and alcohol. In the temperature range of 700-750 °C, the weight of the sample decreases quickly, which may result from the complicated reactions of lithium carbonate, and titanium oxide compounds. This is supported by sharp peak observed at 720 °C on the DTG curve. The weight of the sample keeps nearly constant when the temperature is above 750 °C. The sheer weight loss which occurs between 750 and 950 °C in the TG curve can be ascribed to the formation of crystalline $\text{Li}_4\text{Ti}_5\text{O}_{12}$. At higher temperature a weight loss is very small negligible of 0.2% between 950 and 1000 °C has been determined. The transitions at the higher temperature indicate that these are associated with consolidation and crystallization of the materials.

X-ray diffraction

The x-ray diffraction patterns of $\text{Li}_4\text{Ti}_5\text{O}_{12}$ calcined at different temperatures are shown in Figure 2. A typical x-ray diffraction (XRD) pattern of $\text{Li}_4\text{Ti}_5\text{O}_{12}$ material and all the diffraction peaks were indexed as spinel $\text{Li}_4\text{Ti}_5\text{O}_{12}$ with the $\text{Fd}3\text{m}$ space group²⁰. XRD patterns for the LTO samples calcined at different temperatures from 850 °C to 950 °C indicated as LTO-1, LTO-2, LTO-3 and LTO-4 are shown in Figure 2. The XRD patterns of the synthesized pure LTO-1 sample intensity peaks which are suppressed and some of the peaks are disappeared because of impurity phase rutile TiO_2 . In contrast, the patterns of the samples synthesized samples at, LTO-2, LTO-3 and LTO-4 are closely in accordance with the $\text{Li}_4\text{Ti}_5\text{O}_{12}$ cubic spinel phase structure. Above 850 °C/16h (LTO-2), TiO_2 and Li_2CO_3 phases react to form pure spinel-phase $\text{Li}_4\text{Ti}_5\text{O}_{12}$ (JCPDS card# 49-0207) by solid-state reaction. No characteristic peaks are observed for other impurities, namely rutile and anatase TiO_2 , when the treating temperature was further enhanced to 900 °C indicating the high purity of the sample. Previous results indicated that, spinel LTO was synthesized by solid-state reaction at 800-1000 °C for 5-24 h^{20,22-23}. When the temperature was enhanced to 950 °C, the $\text{Li}_4\text{Ti}_5\text{O}_{12}$ began to decompose, the broad peaks with weak intensities indicate

the poor crystallinity of the formed precursor, which was in accordance with the TG-DTG results. It can be observed from the XRD pattern the sample that all the peaks can be indexed to the cubic spinel-phase. The crystalline size (D) of $\text{Li}_4\text{Ti}_5\text{O}_{12}$ was determined from the Bragg peaks using Scherrer's formula: $D = \frac{k\lambda}{\beta \cos \theta}$.

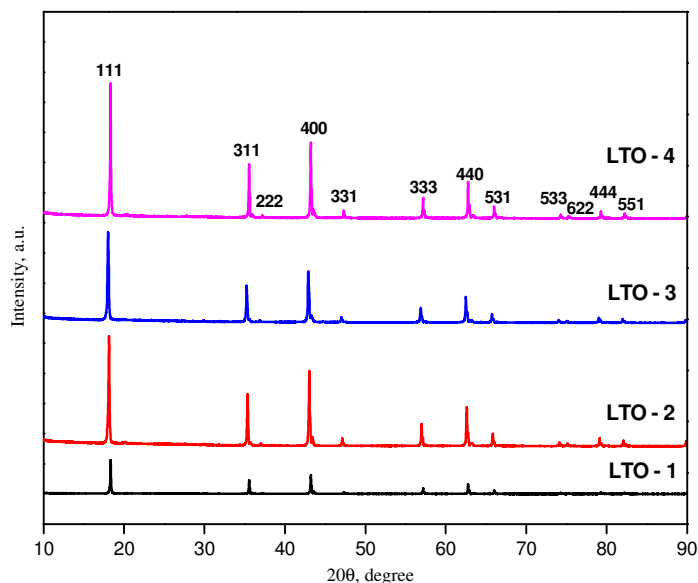


Figure 2. XRD patterns of the $\text{Li}_4\text{Ti}_5\text{O}_{12}$ calcined at different temperatures

Where D is the crystallite size, k is the shape factor taken as 0.9, λ is the wavelength of the x-ray radiation (0.15418 nm for Cu-K α), θ is the Bragg's angle and β is the full width at half maximum (FWHM) of the diffraction peak measured at 2θ in radians²¹. The calculated crystalline sizes of the LTO-1, LTO-2, LTO-3 and LTO-4 samples from line broadening of the most intense diffraction peaks (1 1 1) planes are 64.40, 46.01, 41.93 and 60.22 nm, respectively. The crystallographic unit cell parameter values are calculated by using the Unit cell software deduced through least squares refinement of these XRD pattern yielded cell parameter values a , consistent with the literature reports as listed in Table 1.

SEM and EDS analysis

In order to investigate the effect of the calcination temperature on the particle size and the morphology are observed by the scanning electron microscope. The SEM images of the synthesized LTO-1, LTO-2, LTO-3 and LTO-4 powders shown in Figure 3(a-d).

These fine $\text{Li}_4\text{Ti}_5\text{O}_{12}$ powders can be attributed to solid state route in which an atomic level mixing of elements is achieved. From Figures 3(a) and 3(b) it can be seen that the pure LTO sample appears as heavily aggregated micron-sized particles of 1.4 and 1.5 μm . The specific results are listed in Table 1. We assume that these densely agglomerated particles can make the Li^+ insertion/extraction in individual $\text{Li}_4\text{Ti}_5\text{O}_{12}$ grains inhomogeneous. The $\text{Li}_4\text{Ti}_5\text{O}_{12}$ grains inside the densely packed particles might be inactive especially during cycle at high current densities due to the increased Li^+ diffusion distance. It is found that when the synthesis temperature increases, particle size becomes shrink. From Figures 3(c-d) samples, the average particle sizes of $\text{Li}_4\text{Ti}_5\text{O}_{12}$ powders are 0.91 and 0.92 μm . Specially, the

small difference of the particle size can be observed in the micrographs with high magnification due to the variation of calcination temperature. The average particle size of the compounds are listed in Table 1.

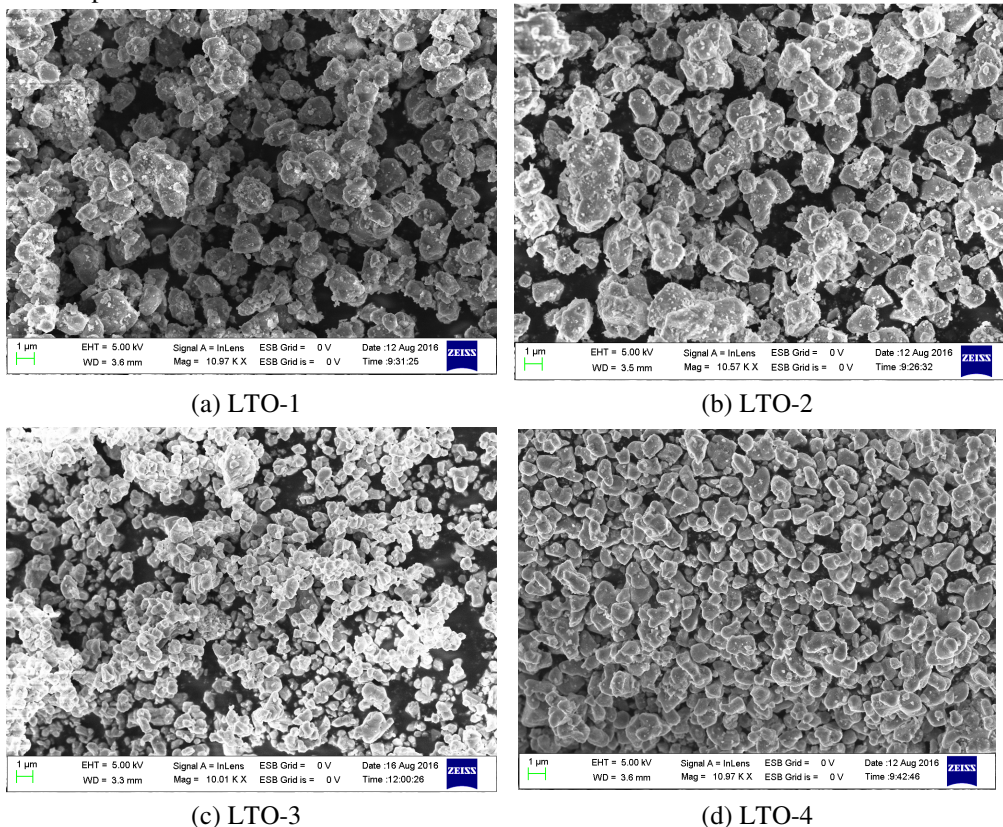


Figure 3(a-d). SEM images for $\text{Li}_4\text{Ti}_5\text{O}_{12}$ calcined at different temperatures

Table 1. Comparison of calcined time, lattice parameter, crystalline size and average particle size of LTO powders

Sample	Calcined time, h	Lattice parameter a (Å)	Cell volume V (Å) ³	Crystalline size, nm	Average particle size, μm
LTO-1	12	8.365	585.43	64.40	1.59
LTO-2	16	8.394	591.38	46.01	1.40
LTO-3	16	8.411	595.09	41.93	0.92
LTO-4	16	8.366	585.58	60.22	0.91

EDS analysis

An energy dispersive spectrum (EDS) is a technique used for the compositional analysis of a material. The EDS spectra confirmed the presence of Ti and O in LTO anode material is show in Figure 4. It is clearly observed that the spectra show the appropriate ratios of the atomic and elements percentage are shown in Table 2. Lithium is not observed in the EDS spectrum because it has too low of an atomic number to be detected with EDS.

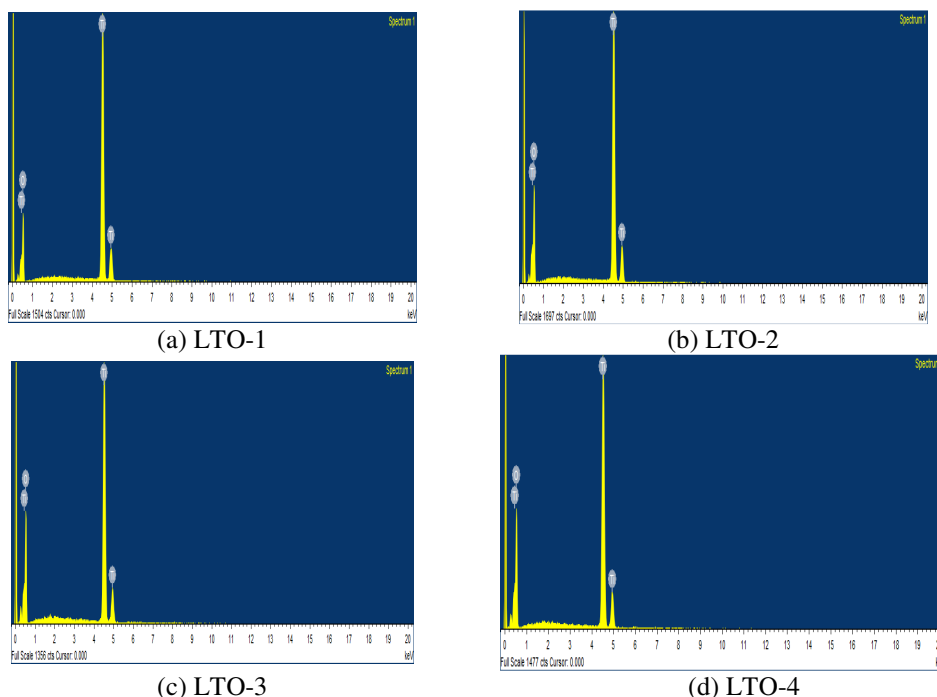


Figure 4(a-d). EDS images for $\text{Li}_4\text{Ti}_5\text{O}_{12}$ calcined at different temperatures

FT-IR analysis

The FT-IR spectra of the synthesized sample LTO prepared by solid state reaction method calcined at different temperature are shown in Figure 5. In order to validate the results of XRD analysis, the room temperature FT-IR spectra of the synthesized sample was performed. The spectra of all synthesized samples do not show much change with variation in calcination temperature. Two distinct peaks are observed in each FT-IR spectrum at different wavelength regions. The two relatively strong frequency bands appeared at wave numbers around 1437 and 1500 cm^{-1} for LTO-4, LTO-3, LTO-2 and LTO-1, are responsible for the formation of $\text{Li}_4\text{Ti}_5\text{O}_{12}$ which might be attributed to asymmetric stretching modes of $\text{Li-Ti-O}^{24,25}$.

Table 2. Elemental analysis and percentage of elements

Sample	Element	Weight%	Atomic%
LTO-1	O	56.95	79.84
	Ti	43.05	20.16
	Total	100	100
LTO-2	O	57.16	79.98
	Ti	42.84	20.02
	Total	100	100
LTO-3	O	47.61	73.13
	Ti	52.39	26.87
	Total	100	100
LTO-4	O	53.31	77.37
	Ti	46.69	22.63
	Total	100	100

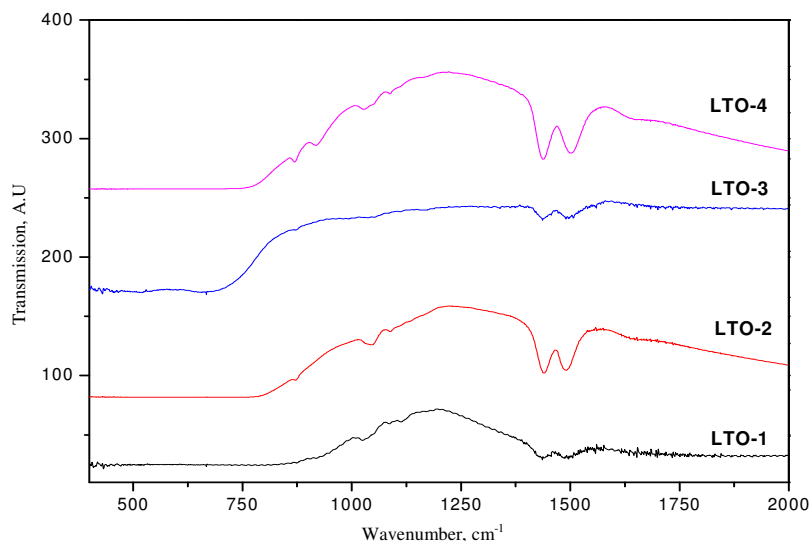


Figure 5. FT-IR spectra of LTO samples

Conclusion

Spinel structure anode material $\text{Li}_4\text{Ti}_5\text{O}_{12}$ was synthesized by solid state reaction method and effect of calcinations temperature on structural characteristics was investigated. In order to investigate the possible reactions occurring in the synthesis of $\text{Li}_4\text{Ti}_5\text{O}_{12}$, thermo gravimetric analysis is conducted on the precursor in N_2 atmosphere. From x-ray diffraction analysis typical x-ray diffraction (XRD) pattern of $\text{Li}_4\text{Ti}_5\text{O}_{12}$ material and all the diffraction peaks were indexed as spinel $\text{Li}_4\text{Ti}_5\text{O}_{12}$ with the $\text{Fd}3\text{m}$ space group. The SEM morphology shows a very fine surface morphology and the crystal grains. The EDS spectra confirmed the presence of Ti and O in $\text{Li}_4\text{Ti}_5\text{O}_{12}$ anode material. The two strong frequency bands appeared at wave numbers 1437 and 1500 cm^{-1} are responsible for the formation of $\text{Li}_4\text{Ti}_5\text{O}_{12}$ which might be attributed to asymmetric stretching modes of Li-Ti-O. From this study we conclude that Spinel $\text{Li}_4\text{Ti}_5\text{O}_{12}$ anode synthesized by solid-state reaction method at different temperature is that the maximum and minimum intensity ratios of XRD spectra shows that the optimum calcinations condition is 900 $^{\circ}\text{C}$ for 16 h.

References

1. Minami T, Tatsumisago M, Wakihara M, Iwakura C, Kohjiya S and Tanaka I, *Solid State Ionics for Batteries*: Springer, 2005.
2. Ohzuku T, Ueda A and Yamamoto V, *J Electrochem Soc.*, 1995, **142**(5), 1431-1435; DOI:10.1149/1.2048592
3. Tarascon J M and Armand M, *Nature*, 2001, **414**, 359-367; DOI:10.1038/35104644
4. Dunn B, Kamath H and Tarascon J M, *Science*, 2011, **334**, 928-935; DOI:10.1126/science.1212741
5. Sato K, Noguchi M, Demachi A, Oki N and Endo M, *Science*, 1994, **264**, 556-558; DOI:10.1126/science.264.5158.556
6. Guo Y G, Hu J S and Wan L J, *Adv Mater.*, 2008, **20**(15), 2878-2887; DOI:10.1002/adma.200800627
7. Winter M and Besenhard J O, *Electrochim Acta*, 1999, **45**(1-2), 31-50; DOI:10.1016/S0013-4686(99)00191-7

8. Winter M, Besenhard J O, Spahr M E and Novak P, *Adv Mater.*, 1998, **10**(10), 725-763; DOI:10.1002/(SICI)1521-4095(199807)10:10<725::AID-ADMA725>3.0.CO;2-Z
9. Idota Y, Kubota T, Matsufuji A, Maekawa Y and Miyasaka T, *Science*, 1997, **276**(5317), 1395-1397; DOI:10.1126/science.276.5317.1395.
10. Chan C K, Peng H, Liu G, McIlwrath K, Zhang X F, Huggins R A and Cui Y, *Nat Nanotech*, 2008, **3**(1), 31-35; DOI:10.1038/nnano.2007.411
11. Poizot P, Laruelle S, Grugeon S, Dupont L and Tarascon J M, *Nature*, 2000, **407**, 496-499; DOI:10.1038/35035045
12. Wang Z, Zhou L and Lou X W, *Adv Mater.*, 2012, **24**(14), 1903-1911; DOI:10.1002/adma.201200469
13. Taberna P L, Mitra S, Poizot P, Simon P and Tarascon J M, *Nat Mater.*, 2006, **5**, 567-573; DOI:10.1038/nmat1672
14. Shaju K M, Jiao F, Debart A and Bruce P G, *Phys Chem Chem Phys.*, 2007, **9**, 1837-1842; DOI:10.1039/B617519H
15. Wang B, Chen J S, Wu H B, Wang Z Y and Lou X W, *J Am Chem Soc.*, 2011, **133**(43), 17146-17148; DOI:10.1021/ja208346s
16. Bresser D, Paillard E, Binetti E, Krueger S, Striccoli M, Winter M and Passerini S, *J Power Sources.*, 2012, **206**, 301-309; DOI:10.1016/j.jpowsour.2011.12.051
17. Poopathy Kathirgamanathan and Muhammad M B Qayyum, *J Electrochem Soc.*, 1994, **141**(1), 147-150; DOI:10.1149/1.2054674
18. Scharner S, Weppner W and Schmid-Beurmann P, *J Electrochem Soc.*, 1999, **146**(3), 857-861; DOI:10.1149/1.1391692
19. Zaghib K, Simoneau M, Armand M and Gauthier M, *J Power Sources*, 1999, **81-82**, 300-305; DOI:10.1016/S0378-7753(99)00209-8
20. Yi T F, Yang S Y and Xie Y, *J Mater Chem A*, 2015, **3**, 5750-5777; DOI:10.1039/C4TA06882C
21. Wang J, Liu X and Yang H, *Trans Nonferrous Met Soc China*, 2012, **22**(3), 613-620; DOI:10.1016/S1003-6326(11)61222-3
22. Qian Y, Hailei Z, Jie W, Jing W, Chunmei W and Xinmei H, *Mater Renew Sustain Energy*, 2014, **3**, 24; DOI:10.1007/s40243-014-0024-7
23. Veljkovic I, Poleti D, Karanovic L J, Zdujic M and Brankovic G, *Sci Sinter.*, 2011, **43**, 343-351; DOI:10.2298/SOS1103343V
24. Prosini P P, Mancini R, Petrucci L, Contini V and Villano V, *Solid State Ionics*, 2001, **144**(1-2), 185-192; DOI:10.1016/S0167-2738(01)00891-8
25. Juan Li, Yong L J, Xiao G Zhang and Yang H, *Solid State Ionics*, 2007, **178**(29-30), 1590-1594; DOI:10.1016/j.ssi.2007.10.012